



blood

2002 99: 1745-1757
doi:10.1182/blood.V99.5.1745

Global gene expression profiling of multiple myeloma, monoclonal gammopathy of undetermined significance, and normal bone marrow plasma cells

Fenghuang Zhan, Johanna Hardin, Bob Kordsmeier, Klaus Bumm, Mingzhong Zheng, Erming Tian, Ralph Sanderson, Yang Yang, Carla Wilson, Maurizio Zangari, Elias Anaissie, Christopher Morris, Firas Muwalla, Frits van Rhee, Athanasios Fassas, John Crowley, Guido Tricot, Bart Barlogie and John Shaughnessy, Jr

Updated information and services can be found at:

<http://www.bloodjournal.org/content/99/5/1745.full.html>

Articles on similar topics can be found in the following Blood collections

[Neoplasia](#) (4212 articles)

Information about reproducing this article in parts or in its entirety may be found online at:

http://www.bloodjournal.org/site/misc/rights.xhtml#repub_requests

Information about ordering reprints may be found online at:

<http://www.bloodjournal.org/site/misc/rights.xhtml#reprints>

Information about subscriptions and ASH membership may be found online at:

<http://www.bloodjournal.org/site/subscriptions/index.xhtml>

Global gene expression profiling of multiple myeloma, monoclonal gammopathy of undetermined significance, and normal bone marrow plasma cells

Fenghuang Zhan, Johanna Hardin, Bob Kordsmeier, Klaus Bumm, Mingzhong Zheng, Erming Tian, Ralph Sanderson, Yang Yang, Carla Wilson, Maurizio Zangari, Elias Anaissie, Christopher Morris, Firas Muwalla, Frits van Rhee, Athanasios Fassas, John Crowley, Guido Tricot, Bart Barlogie, and John Shaughnessy Jr

Bone marrow plasma cells (PCs) from 74 patients with newly diagnosed multiple myeloma (MM), 5 with monoclonal gammopathy of undetermined significance (MGUS), and 31 healthy volunteers (normal PCs) were purified by CD138⁺ selection. Gene expression of purified PCs and 7 MM cell lines were profiled using high-density oligonucleotide microarrays interrogating about 6800 genes. On hierarchical clustering analysis, normal and MM PCs were differentiated and 4 distinct subgroups of MM (MM1, MM2, MM3, and MM4) were identified. The expression pattern of MM1 was similar to normal PCs

and MGUS, whereas MM4 was similar to MM cell lines. Clinical parameters linked to poor prognosis, abnormal karyotype ($P = .002$) and high serum β_2 -microglobulin levels ($P = .0005$), were most prevalent in MM4. Also, genes involved in DNA metabolism and cell cycle control were overexpressed in a comparison of MM1 and MM4. In addition, using χ^2 and Wilcoxon rank sum tests, 120 novel candidate disease genes were identified that discriminate normal and malignant PCs ($P < .0001$); many are involved in adhesion, apoptosis, cell cycle, drug resistance, growth arrest, oncogenesis, signal-

ing, and transcription. A total of 156 genes, including *FGFR3* and *CCND1*, exhibited highly elevated ("spiked") expression in at least 4 of the 74 MM cases (range, 4-25 spikes). Elevated expression of these 2 genes was caused by the translocation t(4;14)(p16;q32) or t(11;14)(q13;q32). Thus, novel candidate MM disease genes have been identified using gene expression profiling and this profiling has led to the development of a gene-based classification system for MM. (Blood. 2002;99:1745-1757)

© 2002 by The American Society of Hematology

Introduction

Progress in understanding the biology and genetics of and advancing therapy for multiple myeloma (MM) has been slow. MM cells are endowed with a multiplicity of antiapoptotic signaling mechanisms, which account for their resistance to current chemotherapy and thus the ultimately fatal outcome for most patients.¹ Although aneuploidy by interphase fluorescence in situ hybridization (FISH)² and DNA flow cytometry³ is observed in more than 90% of cases, cytogenetic abnormalities in this typically hypoproliferative tumor are informative in only about 30% of cases and are typically complex, involving on average 7 different chromosomes. Given this "genetic chaos," it has been difficult to establish correlations between genetic abnormalities and clinical outcomes.^{4,5} Only recently has chromosome 13 deletion been identified as a distinct clinical entity with a grave prognosis.⁶⁻⁸ However, even with the most comprehensive analysis of laboratory parameters, such as β_2 -microglobulin (β_2M),⁹ C-reactive protein,¹⁰ plasma cell labeling index,¹¹ metaphase karyotyping,^{7,8} and FISH,¹²⁻¹⁴ the clinical course of patients afflicted with MM can only be approximated, because no more than more than 20% of the clinical heterogeneity can be accounted for.⁷

The advent of high-density oligonucleotide DNA microarray has made possible a simultaneous analysis of messenger RNA (mRNA) expression patterns of thousands of genes pertinent to

various biologic functions.¹⁵ Here we report that, in a comparison with normal plasma cells (PCs), MM PCs are distinctly different. Furthermore, using hierarchical clustering, 4 distinct subgroups of MM PCs were established that reveal significant correlations with clinical characteristics known to be associated with poor prognosis. This system represents the framework for a new classification system and identifies the genetic differences associated with these distinct subgroups.

Materials and methods

Cell collection and total RNA purification

Samples included PCs from 74 newly diagnosed cases of MM, 5 patients with monoclonal gammopathy of undetermined significance (MGUS), and 31 healthy donors (normal PCs). Written informed consent was obtained in keeping with institutional policies. PC isolation from mononuclear cell fraction was performed by immunomagnetic bead selection with monoclonal mouse antihuman CD138 antibodies using the AutoMACs automated separation system (Miltenyi-Biotec, Auburn, CA). PC purity of more than 95% homogeneity was confirmed by 2-color flow cytometry using CD138⁺/CD45⁻ and CD38⁺/CD45⁻ criteria (Becton Dickinson, San Jose, CA), immunocytochemistry for cytoplasmic light-chain immunoglobulin (Ig), and morphology by Wright-Giemsa staining. MM cell lines (U266, ARP1,

From the Donna D. and Donald M. Lambert Laboratory of Myeloma Genetics, Myeloma Institute for Research and Therapy, or Department of Pathology, University of Arkansas for Medical Sciences, Little Rock, and the Southwest Oncology Group, Fred Hutchinson Cancer Research Center, Seattle, WA.

Submitted June 6, 2001; accepted October 23, 2001.

Supported by private funding from Donna D. and Donald M. Lambert and grant no. CA55819 from the National Cancer Institute, Bethesda, MD.

Reprints: John D. Shaughnessy Jr, Donna D. and Donald M. Lambert Laboratory of Myeloma Genetics, University of Arkansas for Medical Sciences, 4301 W Markham St, Slot 776, Little Rock, AR 72205; e-mail: shaughnessyjohn@uams.edu.

The publication costs of this article were defrayed in part by page charge payment. Therefore, and solely to indicate this fact, this article is hereby marked "advertisement" in accordance with 18 U.S.C. section 1734.

© 2002 by The American Society of Hematology

RPMI-8226, UUN, ANBL-6, CAG, and H929 [courtesy of P. L. Bergsagel] and an Epstein-Barr virus (EBV)-transformed B-lymphoblastoid cell line (ARH-77) were grown as recommended (American Type Culture Collection, Chantilly, VA). Total RNA was isolated with RNeasy Mini Kit (Qiagen, Valencia, CA). The entire Affymetrix data set of all 118 PC samples can be found at <http://lambertlab.uams.edu>.

Preparation of labeled complementary RNA and hybridization to high-density microarray

Double-stranded complementary DNA (cDNA) and biotinylated complementary RNA (cRNA) were synthesized from total RNA and hybridized to HuGeneFL GeneChip microarrays (Affymetrix, Santa Clara, CA), which were washed and scanned according to procedures developed by the manufacturer. The arrays were scanned using Hewlett Packard confocal laser scanner and visualized using Affymetrix 3.3 software (Affymetrix). Arrays were scaled to an average intensity of 1500 and analyzed independently. Technical details of this analysis are available via the Internet at <http://lambertlab.uams.edu>.

GeneChip data analysis

To efficiently manage and mine high-density oligonucleotide DNA microarray data, a new data-handling tool was developed. GeneChip-derived expression data were stored on an MS SQL Server. This database was linked, via an MS Access interface called Clinical Gene-Organizer to multiple clinical parameter databases for patients with MM. This Data Mart concept allows gene expression profiles to be directly correlated with clinical parameters and clinical outcomes using standard statistical software. An MS JET version of Clinical Gene-Organizer can be downloaded from our Web page at <http://lambertlab.uams.edu>. All data used in our analysis were derived from Affymetrix 3.3 software. GeneChip 3.3 output files are given (1) as an average difference (AD) that represents the difference between the intensities of the sequence-specific perfect match probe set and the mismatch probe set, or (2) as an absolute call (AC) of present or absent as determined by the GeneChip 3.3 algorithm. AD calls were transformed by the natural log after substituting any sample with an AD of less than 60 with the value 60 (2.5 times the average Raw Q). Statistical analyses of the data were performed with software packages SPSS 10.0 (SPSS, Chicago, IL), S-Plus 2000 (Insightful, Seattle, WA), and Gene Cluster/Treeview.¹⁶

Hierarchical clustering of average linkage clustering with the centered correlation metric was used.¹⁶ The clustering was done on the AD data of 5483 genes. Either χ^2 or Fisher exact test was used to find significant differences between cluster groups with the AC data. To compare the expression levels, the nonparametric Wilcoxon rank sum (WRS) test was used. This test uses a null hypothesis that is based on ranks rather than on normally distributed data. Before the above tests were performed, genes that were absent (AC) across all samples were removed; 5483 genes were used in the analyses. Genes that were significant ($P < .0001$) for both the χ^2 test and the WRS test were considered to be significantly differentially expressed.

Clinical parameters were tested across MM cluster groups. To test the continuous variables, we used an ANOVA test; to test discrete variables, a χ^2 test of independence or Fisher exact test was applied.

The natural logs of the AD data were used to find genes with a "spiked profile" of expression in MM. Genes were identified that had low to undetectable expression in the majority of patients and normal samples (no more than 4 present absolute calls [P-ACs]). A total of 2030 genes fit the criteria of this analysis. The median expression value of each of the genes across all patient samples was determined. For the i^{th} gene, we called this value *medgene* (*i*). We called the i^{th} gene a "spiked" gene if it had at least 4 patient expression values more than $2.5 + \text{medgene} (i)$. The constant 2.5 was based on the log of the AD data. These genes that were "spiked" were further divided into subsets according to whether or not the largest spike had an AD expression value more than 10 000.

Reverse transcription-polymerase chain reaction

Reverse transcription-polymerase chain reaction (RT-PCR) for the *FGFR3* MMSET was performed on the same cDNAs used in the microarray analysis. Briefly, cDNA was mixed with the IGJH2 (5'-CAATGGTCAC-CGTCTCTTCA-3') primer and the MMSET primer (5'-CCTCAATTCCT-GAAATTGGTT-3'). PCR reactions consisted of 30 cycles with a 58°C annealing temperature and 1-minute extension time at 72°C using a Perkin-Elmer GeneAmp 2400 thermocycler (Wellesley, MA). PCR products were visualized by ethidium bromide staining after agarose gel electrophoresis.

Immunohistochemistry

Immunohistochemical staining was performed on a Ventana ES (Ventana Medical Systems, Tucson, AZ) using Zenker-fixed paraffin-embedded bone marrow sections, an avidin-biotin peroxidase complex technique (Ventana Medical Systems), and the antibody L26 (CD20, Ventana Medical Systems). Heat-induced epitope retrieval was performed by microwaving the sections for 28 minutes in a 1.0-mmol/L concentration of citrate buffer at pH 6.0.

Interphase FISH

For interphase detection of the t(11;14)(q13;q32) translocation fusion signal, we used a the LSI IGH/CCND1 dual-color, dual-fusion translocation probe (Vysis, Downers Grove, IL). The TRI-FISH procedure used to analyze the samples has been previously described.¹² Briefly, at least 100 clonotypic PCs, identified by cytoplasmic immunoglobulin (cIg) staining were counted for the presence or absence of the translocation fusion signal in all samples except one, which yielded only 35 PCs. An MM sample was defined as having the translocation when more than 25% of the cells contained the fusion.

Flow cytometry

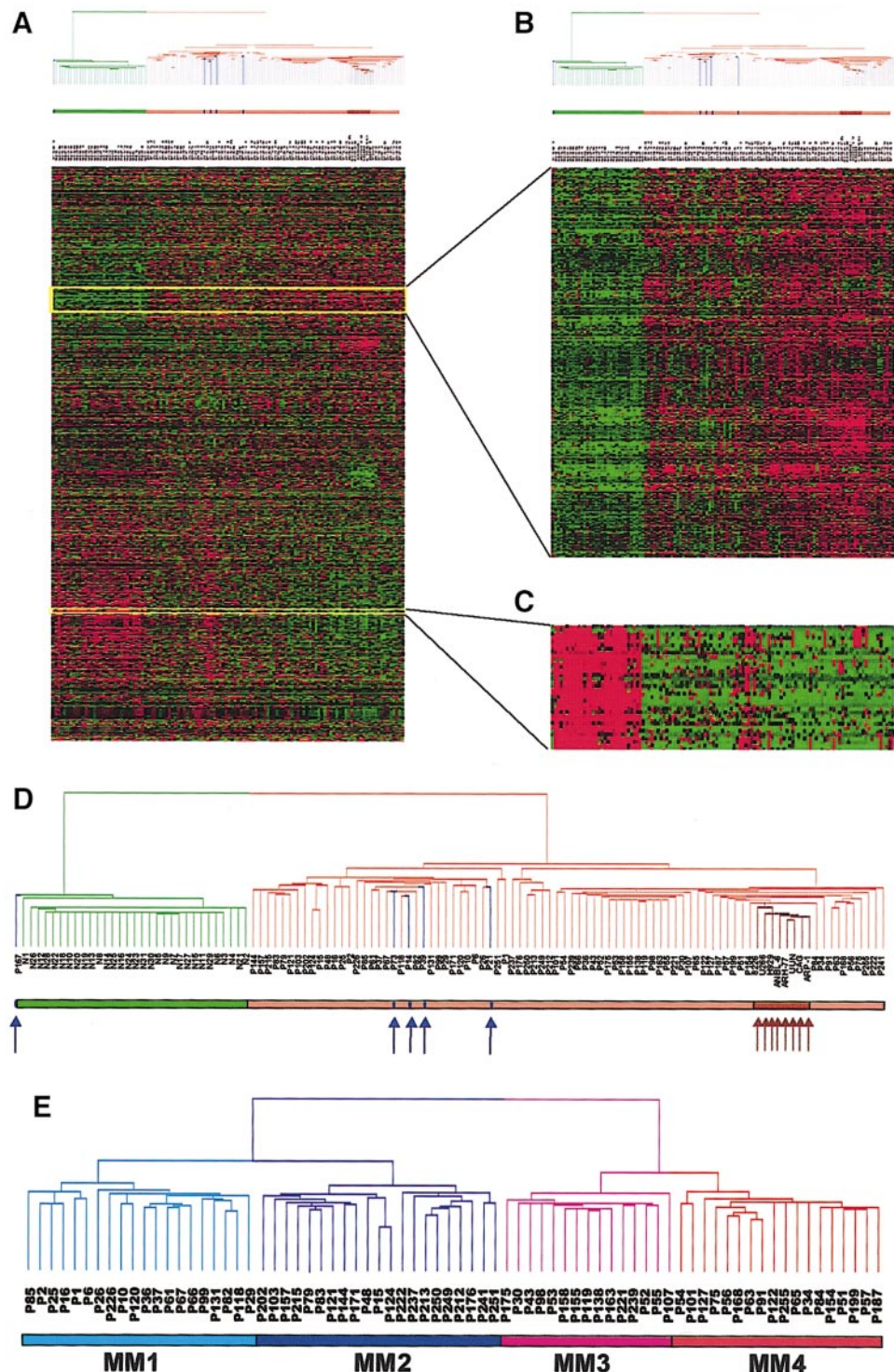
For flow cytometric analysis of CD marker expression, a panel of antibodies directly conjugated to fluorescein isothiocyanate (FITC) or phycoerythrin (PE) was used: FITC-labeled CD19, CD20, and CD22 (Becton Dickinson); CD38 and CD45 (BD Pharmingen, San Diego, CA); CD52 and CD138 (Serotec, Raleigh, NC), and PE-labeled CD21 (BD Pharmingen). Cells were harvested from culture, washed in phosphate-buffered saline (PBS) and stained at 4°C with CD antibodies or isotype-matched control antibodies. After staining, cells were fixed in 1% paraformaldehyde and analyzed using a FACScan flow cytometer (Becton Dickinson).

Results

Hierarchical clustering of PC gene expression demonstrates class distinction

As a result of 656 000 measurements of gene expression in 118 PC samples, altered gene expression in the MM samples was identified. Two-dimensional hierarchical clustering differentiated cell types by gene expression when performed on 5483 genes when expression was present in at least one of the 118 samples (Figure 1A). The sample dendrogram derived 2 major branches (Figure 1A,D). One branch contained all 31 normal samples and a single MGUS case, whereas the second branch contained all 74 MM and 4 MGUS cases and the 8 cell lines. The MM-containing branch was further divided into 2 sub-branches, one containing the 4 MGUS and the other the 8 MM cell lines, which were all clustered next to one another, thus showing a high degree of similarity in gene expression among the cell lines. This suggested that MM could be differentiated from normal PCs and that at least 2 different classes

Figure 1. Two-dimensional hierarchical cluster analysis of experimental expression profiles and gene behavior. (A) Cluster-ordered data table. The clustering is presented graphically as a colored image. Along the vertical axis, the analyzed genes are arranged as ordered by the clustering algorithm. The genes with the most similar patterns of expression are placed adjacent to each other. Likewise, along the horizontal axis, experimental samples are arranged; those with the most similar patterns of expression across all genes are placed adjacent to each other. Both sample and gene groupings can be further described by following the solid lines (branches) that connect the individual components with the larger groups. The color of each cell in the tabular image represents the expression level of each gene, with red representing an expression greater than the mean, green representing an expression less than the mean, and the deeper color intensity representing a greater magnitude of deviation from the mean. (B) Amplified gene cluster showing genes down-regulated in MM. Most of the characterized and sequence-verified cDNA-encoded genes are known to be immunoglobulins. (C) Cluster enriched with genes whose expression level was correlated with tumorigenesis, cell cycle, and proliferation rate. Many of these genes were also statistically significantly up-regulated in MM (χ^2 and WRS test) (Table 5). (D) Dendrogram of hierarchical cluster; 74 cases of newly diagnosed untreated MM, 5 MGUS, 8 MM cell lines, and 31 normal bone marrow PC samples clustered based on the correlation of 5483 genes (probe sets). Different-colored branches represent normal PC (green), MGUS (blue arrow), MM (tan), and MM cell lines (brown arrow). (E) Dendrogram of a hierarchical cluster analysis of 74 cases of newly diagnosed untreated MM alone (clustergram not shown). Two major branches contained 2 distinct cluster groups. The subgroups under the right branch, designated MM1 (light blue) and MM2 (blue) were more related to the MGUS cases in Figure 1D. The 2 subgroups under the left branch, designated MM3 (violet) and MM4 (red) represent samples that were more related to the MM cell lines in Figure 1D.



of MM could be identified, one more similar to MGUS and the other similar to MM cell lines. To show reproducibility of the technique and analysis, we repeated the hierarchical clustering analysis with all 118 samples, including duplicate samples from 12 patients (PCs taken 24 hours or 48 hours after initial sample). All samples from the 12 patients studied longitudinally were found to cluster adjacent to one another. This indicated that gene expression in samples from the same patient were more similar to each other than they were to all other samples (data not shown).

The clustergram (Figure 1A) showed that genes of unrelated sequence but similar function clustered tightly together along the vertical axis. For example, a particular cluster of 22 genes, primarily those encoding immunoglobulin molecules and major histocompatibility genes, had relatively low expression in MM PCs and high expression in normal PCs (Figure 1B). This was anticipated, given that the PCs isolated from MM are clonal and hence only express single immunoglobulin light-chain and heavy-chain variable and constant region genes, whereas PCs from healthy donors are polyclonal and express many

different genes of these 2 classes. Another cluster of 195 genes was highly enriched for numerous oncogenes/growth-related genes (eg, *MYC*, *ABL1*, *PHB*, and *EXT2*), cell cycle-related genes (eg, *CDC37*, *CDK4*, and *CKS2*), and translation machinery genes (*EIF2*, *EIF3*, *HTF4A*, and *TFIIA*) (Figure 1C). These genes were all highly expressed in MM, especially in MM cell lines, but had low expression levels in normal PCs.

Hierarchical clustering of newly diagnosed MM identifies 4 distinct subgroups

We performed 2-dimensional cluster analysis of the 74 MM cases alone. The sample dendrogram identified 2 major branches with 2 distinct subgroups within each branch (Figure 1E). We designated the 4 subgroups MM1, MM2, MM3, and MM4 containing 20, 21, 15, and 18 patients, respectively. The MM1 subgroup represented the patients whose PCs were most closely related to the MGUS PCs and whose MM4 were most like the MM cell lines (Figure 1D). These data suggested that the 4 gene expression subgroups were authentic and might represent 4 distinct clinical entities. We then examined differences in gene expression across the 4 subgroups using the χ^2 and WRS tests (Table 1). As expected the largest difference was between MM1 and MM4 (205 genes) and the smallest between MM1 and MM2 (24 genes). We then looked at the top 30 genes turned on, or up-regulated, in MM4 compared with MM1 (Table 2). These data demonstrated that 13 of the 30 most significant genes (10 of the top 15 genes) were involved in DNA replication/repair or cell cycle control. Thymidylate synthase (*TYMS*), which was present in all 18 samples comprising the MM4 subgroup, was only present in 3 of the 20 MM1 samples and represented the most significant gene in the χ^2 test. The DNA mismatch repair gene, mutS (*Escherichia coli*) homolog 2 (*MSH2*) with a WRS *P* value of 2.8×10^{-6} was the most significant gene in the WRS test. Other notable genes in the list included the CAAX farnesyltransferase (*FNTA*), the transcription factors enhancer of zeste homolog 2 (*EZH2*) and *MYC*-associated zinc finger protein (*MAZ*), eukaryotic translation initiation factors (*EIF2S1* and *EIF2B1*), as well as the mitochondrial translation initiation factor 2 (*MTIF2*), the chaperone (*CCT4*), the UDP-glucose pyrophosphorylase 2 (*IUGP2*), and the 26S proteasome-associated pad1 homolog (*POH1*).

To assess the validity of the clusters with respect to clinical features, correlations of various clinical parameters across the 4 subgroups were analyzed (Table 3). Of 17 clinical variables tested, the presence of an abnormal karyotype (*P* = .0003) and serum β_2 M levels (*P* = .0005) were significantly different among the 4 subgroups and increased creatinine (*P* = .06) and cytogenetic deletion of chromosome 13 (*P* = .09) were marginally significant. The trend was to have higher β_2 M and creatinine as well as an abnormal karyotype and deletion 13 in the MM4 subgroup, as compared with the other 3 subgroups.

Table 1. Differences in gene expression among MM subgroups

Comparison	Range of WRS* <i>P</i>	Number of genes
MM1 vs MM4	.00097 to 9.58×10^{-7}	205
MM2 vs MM4	.00095 to 1.04×10^{-6}	162
MM3 vs MM4	.00098 to 3.75×10^{-6}	119
MM1 vs MM3	.00091 to 6.27×10^{-6}	68
MM2 vs MM3	.00097 to 1.98×10^{-5}	44
MM1 vs MM2	.00083 to 2.93×10^{-5}	24

*Wilcoxon rank sum test. Comparisons are ordered based on the number of significant genes. All comparisons have a WRS *P* < .001.

Altered expression of 120 genes differentiates malignant from normal PCs

Our hierarchical cluster analysis showed that MM PCs could be differentiated from normal PCs. Genes distinguishing the MM from normal PCs were identified as significant by χ^2 analysis and the WRS test (*P* < .0001). A statistical analysis showed that 120 genes distinguished MM from normal PCs. Pearson correlation analyses of the 120 differentially expressed genes were used to identify whether the genes were up-regulated or down-regulated in MM.

When genes associated with immune function (eg, *IGH*, *IGL*, *HLA*), representing the majority of significantly down-regulated genes, were filtered out, 50 genes showed significant down-regulation in MM (Table 4). The *P* values for the WRS test ranged from 9.80×10^{-5} to 1.56×10^{-14} and the χ^2 test of the absence or presence of the expression of the gene in the groups ranged from 18.83 to 48.45. The gene representing the most significant difference in the χ^2 test was the CXC chemokine *SDF1*. It is important to note that a comparison of MM PCs to tonsil-derived PCs showed that, like MM PCs, tonsil PCs also do not express *SDF1* (J.S., manuscript in preparation). Two additional CXC chemokines, *PF4* and *PF4VI*, were also absent in MM PCs. The second most significant gene was the tumor necrosis factor receptor (TNFR) super family member *TNFRF7* coding for CD27, a molecule that has been linked to controlling maturation and apoptosis of plasma cells.¹⁷⁻¹⁹ The largest group of genes, 20 of 50, were linked to signaling cascades. MM PCs have reduced or no expression of genes associated with calcium signaling (*S100A9* and *S100A12*) or lipoprotein signaling (*LIPA*, *LCN2*, *PLA2G7*, *APOE*, *APOC1*). *LCN2*, also known as *24p3*, codes for secreted lipocalin, which has recently been shown to induce apoptosis in pro B-cells after growth factor deprivation.²⁰ Another major class absent in MM PCs was adhesion-associated genes (*ITGA2B*, *IGTB2*, *GP5*, *VCAM*, and *MIC2*).

Correlation analysis showed that 70 genes were either turned on or up-regulated in MM (Table 5). When considering the χ^2 test of whether expression is present or absent, the cyclin-dependent inhibitor, *CDKN1A*, was the most significantly differentially expressed gene ($\chi^2 = 53.33$, WRS = 3.65×10^{-11}). When considering a quantitative change using the WRS test, the tyrosine kinase oncogene *ABL1* was the most significant ($\chi^2 = 43.10$, WRS = 3.96×10^{-14}). Other oncogenes in the list included *USF2*, *USP4*, *MLLT3*, and *MYC*. The largest class of genes represented those whose products are involved in protein metabolism (12 genes), including amino acid synthesis, translation initiation, protein folding, glycosylation, trafficking, and protein degradation. Other multiple-member classes included transcription (11 genes), signaling (9 genes), DNA synthesis and modification (6 genes), and histone synthesis and modification (5 genes). Members of the signaling group included genes whose overexpression has been linked to growth arrest, *QSCN6* and *PHB*, as well as phosphatases, *PTPRK* and *PPP2R4*, and the kinase *MAPKAPK3*. The only secreted growth factor in the signaling class was *HGF*, a factor known to play a role in MM biology.²¹ The *MOX2* gene, whose product is normally expressed as an integral membrane protein on activated T cells and CD19⁺ B cells and is involved in inhibiting macrophage activation, was in the signaling class. The tumor suppressor gene and negative regulator of β -catenin signaling, *APC*, was another member of the signaling class. Classes containing 2 members included RNA binding, mitochondrial respiration, cytoskeletal matrix, metabolism, cell cycle, and adhesion. Single member classes included complement cascade (*MASPI*), drug

Table 2. The 30 most differentially expressed genes in a comparison of MM1 and MM4 subgroups

Accession*	Function	Gene symbol†	MM1 (N = 20) P	MM4 (N = 18) P	χ^2	WRS‡ P value
D00596	DNA replication	<i>TYMS</i>	3	18	24.35	1.26×10^{-4}
U35835	DNA repair	<i>PRKDC</i>	2	17	23.75	4.55×10^{-6}
U77949	DNA replication	<i>CDC6</i>	1	13	15.62	5.14×10^{-6}
U91985	DNA fragmentation	<i>DFFA</i>	1	12	13.38	6.26×10^{-5}
U61145	Transcription	<i>EZH2</i>	4	15	12.77	1.67×10^{-4}
U20979	DNA replication	<i>CHAF1A</i>	2	12	10.75	1.10×10^{-4}
U03911	DNA repair	<i>MSH2</i>	0	9	10.48	2.88×10^{-6}
X74330	DNA replication	<i>PRIM1</i>	0	9	10.48	9.36×10^{-6}
X12517	SnRNP	<i>SNRPC</i>	0	9	10.48	5.26×10^{-6}
D85131	Transcription	<i>MAZ</i>	0	9	10.48	1.08×10^{-5}
L00634	Farnesyltransferase	<i>FNTA</i>	10	18	9.77	7.28×10^{-5}
U21090	DNA replication	<i>POLD2</i>	11	18	8.27	8.05×10^{-5}
X54941	Cell cycle	<i>CKS1</i>	10	17	7.07	1.26×10^{-4}
U62136	Cell cycle	<i>UBE2V2</i>	13	18	5.57	4.96×10^{-6}
D38076	Cell cycle	<i>RANBP1</i>	13	18	5.57	7.34×10^{-6}
X95592	Unknown	<i>C1D†</i>	13	18	5.57	1.10×10^{-4}
X66899	Cell cycle	<i>EWSR1</i>	14	18	4.35	1.89×10^{-4}
L34600	Translation initiation	<i>MTIF2</i>	14	18	4.35	3.09×10^{-5}
U27460	Metabolism	<i>IUGP2</i>	15	18	3.22	1.65×10^{-4}
U15009	SnRNP	<i>SNRPD3</i>	15	18	3.22	1.47×10^{-5}
J02645	Translation initiation	<i>EIF2S1</i>	16	18	2.18	7.29×10^{-5}
X95648	Translation initiation	<i>EIF2B1</i>	16	18	2.18	1.45×10^{-4}
M34539	Calcium signaling	<i>FKBP1A</i>	18	18	0.42	1.71×10^{-5}
J04611	DNA repair	<i>G22P1</i>	18	18	0.42	7.29×10^{-5}
U67122	Antiapoptosis	<i>UBL1</i>	20	18	0.00	7.29×10^{-5}
U38846	Chaperon	<i>CCT4</i>	20	18	0.00	1.26×10^{-4}
U80040	Metabolism	<i>ACO2</i>	20	18	0.00	8.38×10^{-5}
U86782	Proteasome	<i>POH†</i>	20	18	0.00	5.90×10^{-5}
X57152	Signaling	<i>CSNK2B</i>	20	18	0.00	7.29×10^{-5}
D87446	Unknown	<i>KIAA0257†</i>	20	18	0.00	1.26×10^{-5}

*Accession numbers listed are GenBank numbers, except those beginning with "HT," which are provided by the Institute of Genomic Research (TIGR).

†Gene symbol not Human Genome Organisation (HUGO) approved.

‡Wilcoxon rank sum test.

resistance (*MVP*), glycosaminoglycan catabolism, heparin sulfate synthesis (*EXTL2*), and vesicular transport (*TSC1*). Four genes of unknown function were also identified as significantly up-regulated in MM.

Gene expression "spikes" in subsets of MM

A total of 156 genes not identified as differently expressed in the statistical analysis of MM versus normal PCs, yet highly overexpressed in subsets of MM, were also identified. A total of 25 genes with an AD spike more than 10 000 in at least one sample are shown (Table 6). With 27 spikes, the adhesion-associated gene *FBLN2* was the most frequently spiked. The gene for the interferon induced protein 27, *IFI27*, with 25 spikes was the second most frequently spiked gene and contained the highest number of spikes over 10 000 ($n = 14$). The *FGFR3* gene was spiked in 9 of the 74 cases (Figure 2A). It was the only gene for which all spikes were more than 10 000 AD. In fact, the lowest AD value was 18 961 and the highest 62 515, which

represented the highest of all spikes. The finding of *FGFR3* spikes suggested that these spikes were induced by the MM-specific, *FGFR3*-activating t(4;14)(p21;q32) translocation.²² To test this hypothesis, we performed RT-PCR for a t(4;14)(p21;q32) translocation-specific fusion transcript between the *IGH* locus and the gene *MMSET* (data not shown). The translocation-specific transcript was present in all 9 *FGFR3* spike samples but was absent in 5 samples that did not express *FGFR3*. These data suggested that the spike was caused by the t(4;14)(p21;q32) translocation. The *CCND1* gene was spiked with AD values of more than 10 000 in 13 cases. We performed TRI-FISH analysis for the t(11;14)(q13;q32) translocation (Table 7). All 11 evaluable samples were positive for the t(11;14)(q13;q32) translocation by TRI-FISH; 2 samples were not analyzable due to loss of cell integrity during storage. Thus, all *FGFR3* and *CCND1* spikes could be accounted for by the presence of either the t(4;14)(p21;q32) translocation or the t(11;14)(q13;q32) translocation, respectively.

Table 3. Clinical parameters linked to MM subgroups

Clinical parameter	MM subgroups				P
	1	2	3	4	
Abnormal cytogenetics	40.0%	10.5%	53.3%	72.2%	.0017
Average β_2 M (mg/L)	2.81	2.73	4.62	8.81	.00047
Average creatinine (mg/dL)	0.96	1.02	1.32	1.77	.06019

ANOVA, χ^2 , and Fisher exact tests were used to determine significance.

Table 4. The 50 most significantly down-regulated genes in MM in comparison with normal bone marrow PCs

Accession*	Function	Gene symbol†	χ^2	WRS‡ P value
L36033	CXC chemokine	<i>SDF1</i>	48.45	3.05×10^{-12}
M63928	Signaling	<i>TNFRSF7</i>	48.45	6.35×10^{-11}
U64998	Ribonuclease	<i>RNASE6</i>	46.44	2.82×10^{-9}
M20902	Lipoprotein signaling	<i>APOC1</i>	45.62	4.63×10^{-10}
M26602	Immunity	<i>DEFA1</i>	40.75	1.06×10^{-12}
M21119	Immunity	<i>LYZ</i>	40.73	6.24×10^{-10}
M14636	Metabolism	<i>PYGL</i>	39.84	1.15×10^{-10}
M26311	Calcium signaling	<i>S100A9</i>	38.96	3.60×10^{-13}
M54992	Signaling	<i>CD72</i>	36.14	2.40×10^{-9}
X16832	Protein degradation	<i>CTSH</i>	35.26	1.81×10^{-12}
M12529	Lipoprotein signaling	<i>APOE</i>	34.50	3.95×10^{-14}
M15395	Adhesion	<i>ITGB2</i>	34.02	1.74×10^{-13}
Z74616	Extracellular matrix	<i>COL1A2</i>	34.02	8.06×10^{-11}
HT2152	Receptor signaling	<i>CD163</i>	33.01	1.66×10^{-12}
U97105	Pyrimidine metabolism	<i>DPYSL2</i>	32.52	2.22×10^{-10}
U81787	Signaling	<i>WNT10B</i>	32.50	1.77×10^{-5}
HT3165	Receptor tyrosine kinase	<i>AXL</i>	31.36	5.26×10^{-11}
M83667	Transcription	<i>CEBPD</i>	31.19	4.69×10^{-10}
L33930	Receptor signaling	<i>CD24</i>	30.33	1.56×10^{-14}
D83657	Calcium signaling	<i>S100A12</i>	29.91	6.58×10^{-8}
M11313	Proteinase inhibitor	<i>A2M</i>	29.91	1.07×10^{-10}
M31158	Signaling	<i>PRKAR2B</i>	29.91	2.20×10^{-9}
U24577	Lipoprotein signaling	<i>PLA2G7</i>	29.78	2.08×10^{-10}
M16279	Adhesion	<i>MIC2</i>	28.75	8.01×10^{-11}
HT2811	Cell cycle	<i>CDK8</i>	28.32	6.53×10^{-9}
M26167	CXC chemokine	<i>PF4V1</i>	27.35	4.68×10^{-11}
U44111	Metabolism	<i>HNMT</i>	27.24	2.07×10^{-11}
X59871	Transcription	<i>TCF7</i>	26.79	7.16×10^{-10}
X67235	Transcription	<i>HHEX</i>	25.21	2.07×10^{-10}
U19713	Calcium signaling	<i>AIF1</i>	25.21	2.57×10^{-10}
Y08136	Apoptosis	<i>ASM3A†</i>	24.74	3.30×10^{-8}
M97676	Transcription	<i>MSX1</i>	24.58	9.80×10^{-5}
M64590	Housekeeping	<i>GLDC</i>	24.27	4.10×10^{-8}
M20203	Protease	<i>ELA2</i>	24.03	6.36×10^{-12}
M30257	Adhesion	<i>VCAM1</i>	23.42	1.71×10^{-10}
M93221	Mediates endocytosis	<i>MRC1</i>	23.30	1.15×10^{-7}
S75256	Lipoprotein signaling	<i>LCN2</i>	23.30	4.17×10^{-7}
U97188	RNA binding	<i>KOC1†</i>	22.47	5.86×10^{-9}
Z23091	Adhesion	<i>GP5</i>	22.47	7.58×10^{-7}
M34344	Adhesion	<i>ITGA2B</i>	21.99	8.00×10^{-8}
M25897	CXC chemokine	<i>PF4</i>	21.89	1.12×10^{-8}
M31994	Housekeeping	<i>ALDH1A1</i>	21.36	4.86×10^{-9}
Z31690	Lipoprotein signaling	<i>LIPA</i>	20.67	1.50×10^{-9}
S80267	Signaling	<i>SYK</i>	20.42	5.90×10^{-5}
U00921	Signaling	<i>LY117</i>	18.83	1.57×10^{-8}

*Accession numbers listed are GenBank numbers, except those beginning with "HT," which are provided by the Institute of Genomic Research (TIGR).

†Gene symbol not HUGO approved.

‡Wilcoxon rank sum test.

We next determined the distribution of the *FGFR3*, *CST6*, *IFI27*, and *CCND1* spikes within the gene expression–defined MM subgroups (Figure 2). The data showed that whereas *FGFR3* and *CST6* spikes were more likely to be found in MM1 or MM2 ($P < .005$), the spikes for *IFI27* were associated with an MM3 and MM4 distribution ($P < .005$). *CCND1* spikes were not associated with any specific subgroup ($P > .1$). It is noteworthy that both *CST6* and *CCND1* map to 11q13 and had no overlap in spikes. We are currently testing whether *CST6* overexpression is due to a variant t(11;14)(q13;q32) translocation. The 5 spikes for *MS4A2* (CD20) were found in either the MM1 (3 spikes) or MM2 (2 spikes) subgroups (data not shown).

The gene *MS4A2*, which codes for the CD20 molecule, was also found as a spiked gene in 4 cases (Figure 3A). To

investigate whether spiked gene expression correlated with protein expression, we performed immunohistochemistry for CD20 on biopsies from 15 of the 74 MM samples (Figure 3B). All 4 cases that had spiked *MS4A2* gene expression were also positive for CD20 protein expression, whereas 11 that had no *MS4A2* gene expression were also negative for CD20 by immunohistochemistry. To add additional validation to the gene expression profiling, we performed a comparison of CD marker protein and gene expression in the MM cell line CAG and the EBV-transformed lymphoblastoid cell line ARH-77 (Figure 4). The expression of CD138 and CD38 protein and gene expression was high in CAG but absent in ARH-77 cells. On the other hand, expression of CD19, CD20, CD21, CD22, CD45, and CDw52 was found to be strong in ARH-77 and absent in CAG

Table 5. The 70 most significantly up-regulated genes in MM in comparison with normal bone marrow PCs

Accession*	Function	Gene symbol†	χ^2	WRS‡ P
U09579	Cell cycle	<i>CDKN1A</i>	53.33	3.65×10^{-11}
U78525	Amino acid synthesis	<i>EIF3S9</i>	49.99	2.25×10^{-12}
HT5158	DNA synthesis	<i>GMPS</i>	47.11	4.30×10^{-12}
X57129	Histone	<i>H1F2</i>	46.59	5.78×10^{-13}
M55210	Adhesion	<i>LAMC1</i>	45.63	1.34×10^{-9}
L77886	Signaling, phosphatase	<i>PTPRK</i>	45.62	5.42×10^{-10}
U73167	Glycosaminoglycan catabolism	<i>HYAL3</i>	44.78	1.07×10^{-10}
X16416	Oncogene, kinase	<i>ABL1</i>	43.10	3.96×10^{-14}
U57316	Transcription	<i>GCN5L2</i>	43.04	1.36×10^{-12}
Y09022	Protein glycosylation	<i>NOT56L†</i>	42.05	5.53×10^{-10}
M25077	RNA binding	<i>SSA2</i>	41.26	1.69×10^{-7}
AC002115	Mitochondrial respiration	<i>COX6B</i>	41.16	2.16×10^{-8}
Y07707	Transcription	<i>NRF†</i>	37.59	4.79×10^{-10}
L22005	Protein ubiquitination	<i>CDC34</i>	34.50	2.89×10^{-6}
X66899	Transcription	<i>EWSR1</i>	34.39	4.23×10^{-8}
D50912	RNA binding	<i>RBM10</i>	33.93	2.61×10^{-6}
HT4824	Amino acid synthesis	<i>CBS</i>	33.77	1.49×10^{-6}
U10324	Transcription	<i>ILF3</i>	33.33	3.66×10^{-11}
AD000684	Oncogene, transcription	<i>USF2</i>	32.18	7.41×10^{-11}
U68723	Cell cycle	<i>CHES1</i>	31.68	1.03×10^{-6}
X16323	Signaling, growth factor	<i>HGF</i>	30.67	4.82×10^{-9}
U24183	Metabolism	<i>PFKM</i>	30.47	8.92×10^{-10}
D13645	Unknown	<i>KIAA0020†</i>	30.47	7.40×10^{-6}
S85655	Signaling, growth arrest	<i>PHB</i>	29.37	1.32×10^{-8}
X73478	Signaling, phosphatase	<i>PPP2R4</i>	28.32	6.92×10^{-9}
L77701	Mitochondrial respiration	<i>COX17</i>	27.81	1.33×10^{-6}
U20657	Oncogene, proteasome	<i>USP4</i>	27.71	2.31×10^{-6}
M59916	Signaling, DAG signaling	<i>SMPD1</i>	27.49	3.52×10^{-8}
D16688	Oncogene, DNA binding	<i>MLL3</i>	27.24	6.97×10^{-13}
X90392	DNA endonuclease	<i>DNASE1L1</i>	26.98	4.72×10^{-7}
U07424	Amino acid synthesis	<i>FARSL</i>	26.93	1.66×10^{-6}
X54199	DNA synthesis	<i>GART</i>	26.57	9.61×10^{-11}
L06175	Unknown	<i>P5-1†</i>	26.57	5.16×10^{-7}
M55267	Unknown	<i>EVI2A</i>	25.92	3.79×10^{-6}
M87507	Protein degradation	<i>CASP1</i>	25.78	5.46×10^{-7}
M90356	Transcription	<i>BTF3L2</i>	25.78	9.68×10^{-8}
U35637	Cytoskeletal matrix	<i>NEB</i>	25.40	9.15×10^{-6}
L06845	Amino acid synthesis	<i>CARS</i>	25.34	5.39×10^{-8}
U81001	DNA, nuclear matrix attachment	<i>SNURF</i>	24.58	4.54×10^{-5}
U76189	Heparan sulfate synthesis	<i>EXTL2</i>	24.58	7.28×10^{-6}
U53225	Protein trafficking	<i>SNX1</i>	24.48	5.53×10^{-7}
X04366	Protein degradation	<i>CAPN1</i>	24.35	1.26×10^{-9}
U77456	Protein folding	<i>NAP1L4</i>	24.27	4.23×10^{-10}
L42379	Signaling, growth arrest	<i>QSCN6</i>	24.27	1.28×10^{-10}
U09578	Signaling, kinase	<i>MAPKAPK3</i>	24.27	2.35×10^{-9}
Z80780	Histone	<i>H2BFH</i>	24.27	3.44×10^{-12}
HT4899	Oncogene, transcription	<i>MYC</i>	24.27	1.77×10^{-5}
M74088	Signaling, b-catenin regulator	<i>APC</i>	23.94	1.50×10^{-5}
X57985	Histone	<i>H2BFQ</i>	23.90	3.25×10^{-12}
X79882	Drug resistance	<i>MVP</i>	23.47	1.77×10^{-11}
X77383	Protein degradation	<i>CTSO</i>	23.18	4.68×10^{-7}
M91592	Transcription	<i>ZNF76</i>	23.16	1.12×10^{-8}
X63692	DNA methyltransferase	<i>DNMT1</i>	23.12	5.15×10^{-11}
M60752	Histone	<i>H2AFO</i>	21.60	1.46×10^{-8}
M96684	Transcription	<i>PURA</i>	21.25	4.54×10^{-5}
U16660	Metabolism	<i>ECH1</i>	21.18	5.52×10^{-5}
M86737	DNA repair	<i>SSRP1</i>	20.60	2.62×10^{-5}
U35113	Histone deacetylase	<i>MTA1</i>	20.60	6.67×10^{-10}
X81788	Unknown	<i>ICT1</i>	20.42	2.97×10^{-7}
HT2217	Signaling	<i>MUC2A</i>	20.33	2.61×10^{-7}
M62324	Unknown	<i>MRF-1†</i>	20.31	3.98×10^{-9}
U09367	Transcription	<i>ZNF136</i>	20.30	7.72×10^{-9}
X89985	Cytoskeletal matrix	<i>BCL7B</i>	19.81	5.50×10^{-9}
L19871	Transcription repression	<i>ATF3</i>	19.43	1.13×10^{-6}
X69398	Adhesion	<i>CD47</i>	19.16	6.44×10^{-7}

Table 5. The 70 most significantly up-regulated genes in MM in comparison with normal bone marrow PCs (continued)

Accession*	Function	Gene symbol†	χ^2	WRS‡ P
X05323	Signaling, macrophage inhibitor	<i>MOX2</i>	19.16	8.58×10^{-6}
X04741	Protein ubiquitination	<i>UCHL1</i>	19.14	9.76×10^{-5}
D87683	Vesicular transport	<i>TSC1</i>	19.12	6.81×10^{-6}
D17525	Complement cascade	<i>MASP1</i>	18.81	4.05×10^{-7}

*Accession numbers listed are GenBank numbers, except those beginning with "HT," which are provided by the Institute of Genomic Research (TIGR).

†Gene symbol not HUGO approved.

‡Wilcoxon rank sum test.

Table 6. Genes with "spiked" expression in subsets of MM PCs from newly diagnosed patients

Accession*	Function	Gene symbol†	No. of spikes	Spikes greater than 10K	Maximum spike
M64347	Signaling	<i>FGFR3</i>	9	9	62 515
U89922	Immunity	<i>LTB</i>	4	2	49 261
X67325	Interferon signaling	<i>IFI27</i>	25	14	47 072
X59798	Cell cycle	<i>CCND1</i>	6	13	42 814
U62800	Cysteine protease inhibitor	<i>CST6</i>	17	6	36 081
U35340	Eye lens protein	<i>CRYBB1</i>	4	1	35 713
X12530	B-cell signaling	<i>MS4A2</i>	5	5	34 487
X59766	Unknown	<i>AZGP1</i>	18	4	28 523
U58096	Unknown	<i>TSPY</i>	4	1	23 325
U52513	Interferon signaling	<i>IFIT4</i>	5	2	21 078
X76223	Vesicular trafficking	<i>MAL</i>	19	5	20 432
X92689	O-linked glycosylation	<i>GALNT3</i>	4	1	18 344
D17427	Adhesion	<i>DSC3</i>	8	7	17 616
L11329	Signaling	<i>DUSP2</i>	14	1	15 962
L13210	Adhesion, macrophage lectin	<i>LGALS3BP</i>	8	2	14 876
U10991	Unknown	<i>G2†</i>	7	1	14 815
L10373	Integral membrane protein	<i>TM4SF2</i>	4	2	14 506
U60873	Unknown	<i>137308</i>	12	1	12 751
M65292	Complement regulation	<i>HFL1</i>	9	1	12 718
HT4215	Phospholipid transport	<i>PLTP</i>	23	1	12 031
D13168	Growth factor receptor	<i>ENDRB</i>	18	1	11 707
AC002077	Signaling	<i>GNAT1</i>	21	1	11 469
M92934	Growth factor	<i>CTGF</i>	4	1	11 201
X82494	Adhesion	<i>FBLN2</i>	27	7	10 648
M30703	Growth factor	<i>AR</i>	5	1	10 163

*Accession numbers listed are GenBank numbers, except those beginning with "HT," which are provided by the Institute of Genomic Research (TIGR).

†Gene symbol not HUGO approved.

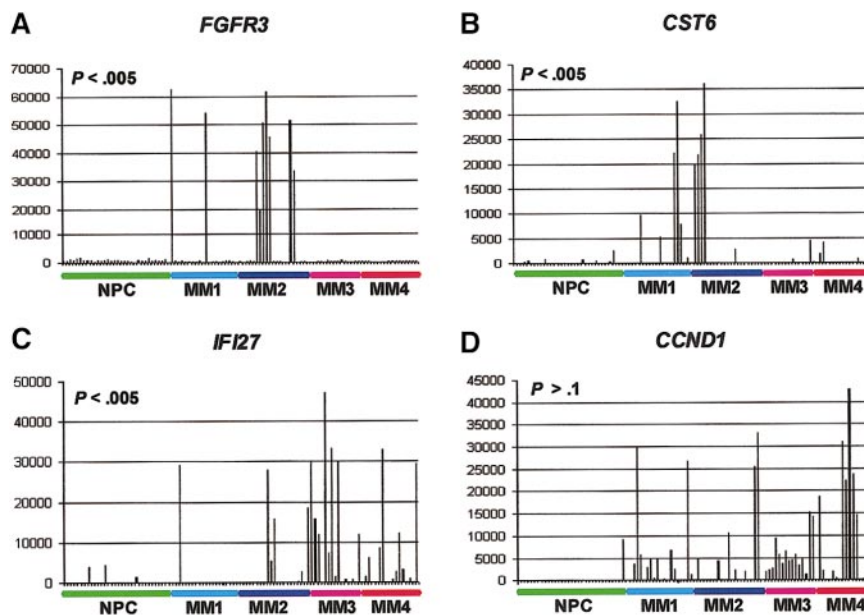


Figure 2. Spike profile distributions among the gene expression-defined MM subgroups. GeneChip HuGeneFL analysis of *FGFR3*, *CST6*, *IFI27*, and *CCND1* gene expression. The normalized AD value of fluorescence intensity of streptavidin-PE-stained biotinylated cRNA as hybridized to probe sets is on the vertical axis and samples are on the horizontal axis. The samples are ordered from left to right: normal PCs (NPCs; green), MM1 (light blue), MM2 (dark blue), MM3 (violet), and MM4 (red). Note relatively low expression in 31 NPCs and spiked expression in subsets of MM samples. The P values of the test for significant nonrandom spike distributions are noted.

cells. The nearly 100% coincidence of *FGFR3* or *CCND1* spiked gene expression with the presence of the t(4;14)(p14;q32) or t(11;14)(q13;q32) translocation, the strong correlation of CD20 and *MS42A* gene expression in primary MM, and CD marker protein and gene expression in B cells and PCs represent important validations of the accuracy of our gene expression profiling.

Discussion

In this report, we have shown that both normal and malignant PCs can be purified to homogeneity from bone marrow aspirates using anti-CD138–based immunomagnetic bead-positive selection. Using these cells we have provided the first comprehensive global gene expression profiling of newly diagnosed MM patients and contrasted these expression patterns with those of normal PCs.

Hierarchical cluster analysis of MM and normal PCs, as well as the benign PC dyscrasia MGUS and the end-stage–like MM cell lines, revealed that normal PCs are unique and that primary MM is either like MGUS or MM cell lines. In addition, MM cell line gene expression was homogeneous as evidenced by the tight clustering in the hierarchical analysis. The similarity of MM cell line expression patterns to primary newly diagnosed forms of MM support the validity of using MM cell lines as models for MM, in particular for our gene expression–defined MM4 subgroup.

On hierarchical clustering of MM alone, 4 MM subgroups were distinguished. Differences indicate that gene expression signatures distinguish distinct clinical entities as (1) the MM1 subgroup contained samples that were more like MGUS (in our first cluster analysis), whereas the MM4 subgroup contained samples more like MM cell lines; (2) the most significant gene expression patterns differentiating MM1 and MM4 were cell cycle control and DNA metabolism genes; and (3) the MM4 subgroup was more likely to have abnormal cytogenetics, elevated serum β_2 M, elevated creatinine, and deletions of chromosome 13—important variables that historically have been linked to poor prognosis.

We speculate that the MM4 subgroup thus likely represents the most high-risk clinical entity. Thus, knowledge of the molecular genetics of this particular subgroup should provide insight into its biology and possibly provide a rationale for appropriate subtype-specific therapeutic interventions. On analysis, the most significant gene expression changes differentiat-

ing the MM1 and MM4 subgroups code for activities that clearly implicate MM4 as having a more proliferative and autonomous phenotype. The most significantly altered gene in the comparison, *TYMS* (thymidylate synthase), which functions in the pyrimidine biosynthetic pathway, has been linked to resistance to fluoropyrimidine chemotherapy and also poor prognosis in colorectal carcinomas.²³ Other notable genes up-regulated in MM4 were the CAAX farnesyltransferase gene, *FTNA*. Farnesyltransferase prenylates RAS, a posttranslational modification required to allow RAS to attach to the plasma membrane. These data suggest that farnesyltransferase inhibitors may be effective in treating patients with high levels of *FTNA* expression. Two genes coding for components of the proteasome pathway, *POHI* (26S proteasome–associated pad1 homolog) and *UBL1* (ubiquitin-like protein 1) were also overexpressed in MM4. Overexpression of *POHI* confers P-glycoprotein–independent, pleiotropic drug resistance to mammalian cells.^{24,25} Given the uniform development of chemotherapy resistance in MM the combined overexpression of *POHI* and *MVP* may have profound influences on this phenotype. In contrast to normal PCs, more than 75% of MM PCs express abundant mRNA for the multidrug resistance gene, lung resistance–related protein (*MVP*). These data are consistent with previous reports showing that expression of *MVP* in MM is a poor prognostic factor.²⁶ Ubiquitin-like protein 1 (*UBL1*) also known as sentrin, is involved in many processes including associating with RAD51, RAD52, and p53 proteins in the double-strand repair pathway²⁷⁻²⁹; conjugating with RANGAP1, involved in nuclear protein import; and importantly for MM, protecting against both Fas/Apo-1 (*TNFRSF6*) or *TNFR1*-induced apoptosis.³⁰ The deregulated expression of many genes whose products function in the proteasome pathway may be used in the pharmacogenomic analysis of efficacy of proteasome inhibitors like PS-341 (Millennium Pharmaceuticals, Cambridge, MA).

Another significantly up-regulated gene in MM4 was the single-stranded DNA-dependent adenosine triphosphate (ATP)–dependent helicase (*G22P1*) also known as Ku70 autoantigen. The DNA helicase II complex, made up of p70 and p80, binds preferentially to forklike ends of double-stranded DNA in a cell cycle–dependent manner. Binding to DNA is thought to be mediated by p70 and dimerization with p80 forms the ATP-dependent DNA-unwinding enzyme (helicase II) and acts as the regulatory component of a DNA-dependent protein kinase (*DNPK*), which was also significantly up-regulated in MM4. The involvement of the helicase II complex in DNA double-strand break repair, V(D)J recombination, and notably chromosomal translocations has been proposed. Another gene up-regulated was the DNA fragmentation factor, 45 kd, alpha (*DFFA*). Caspase-3 cleaves the *DFFA*-encoded 45-kd subunit at 2 sites to generate an active factor that produces DNA fragmentation during apoptosis signaling. We speculate that, in light of the many blocks to apoptosis in MM, *DFFA* activation could result in DNA fragmentation, which in turn would activate the helicase II complex that then may facilitate chromosomal translocations. It is of note that abnormal karyotypes, and thus chromosomal translocations, are associated with the MM4 subgroup, which tended to overexpress these 2 genes.

A direct comparison of gene expression patterns in MM and normal PCs identified novel genes with highly significant differences that could represent the fundamental changes associated with the malignant transformation of PCs.

Table 7. Correlation of *CCND1* spikes with FISH-defined t(11;14)(q13;q32)

GC PT	<i>CCND1</i> spike (AD value)	FISH t(11;14)	% PCs with translocation	Cells counted
P168	42 813	Yes	59	113
P251	33 042	Yes	80	124
P91	31 030	Not done	—	—
P99	29 862	Yes	65	111
P85	26 737	Yes	92	124
P241	25 611	Yes	96	114
P56	23 654	Yes	100	106
P63	22 358	Yes	98	104
P199	18 761	Yes	60	35
P107	15 205	Yes	100	147
P75	14 642	Yes	100	105
P187	14 295	Yes	25	133
P124	10 594	Not done	—	—

GC PT indicates patient identifier; AD, average difference call.

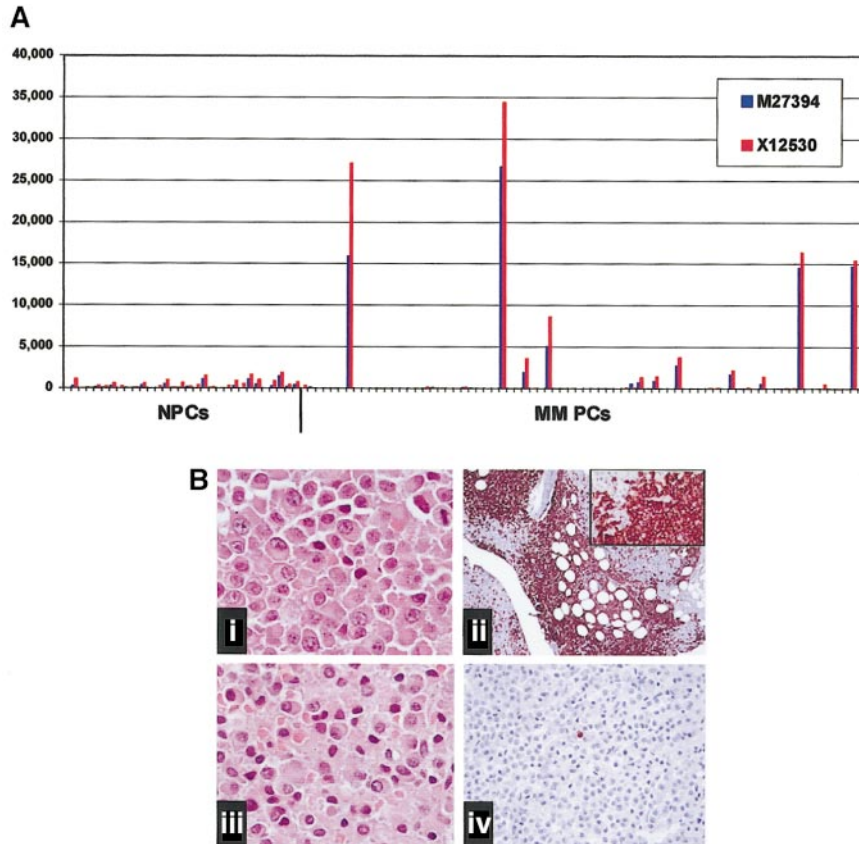
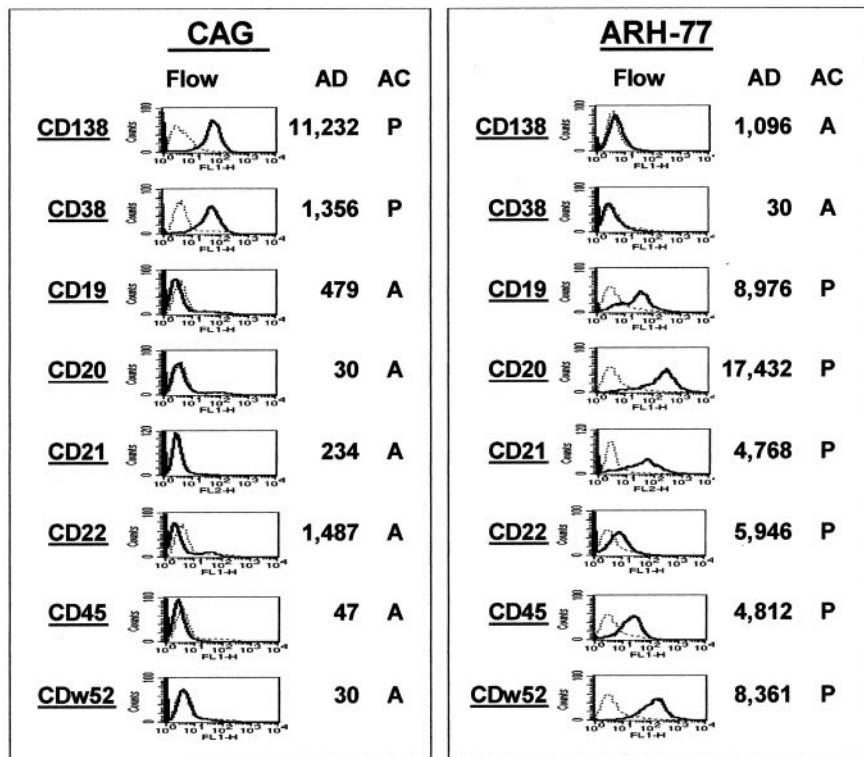


Figure 3. Spiked gene expression corresponds to protein expression in MM. (A) GeneChip HuGeneFL analysis of *MS4A2* (*CD20*) gene expression. The normalized AD value of fluorescence intensities of streptavidin-PE-stained biotinylated cRNA as hybridized to 2 independent probe sets (accession numbers M27394 [blue] and X12530 [red]) located in different regions of the *MS4A2* gene is on the vertical axis and samples are on the horizontal axis. Note relatively low expression in 31 normal PCs (NPCs) and spiked expression in 5 of 74 MM samples (MM PCs). Also note similarity in expression levels detected by the 2 different probe sets. (B) Immunohistochemistry for *CD20* expression on clonal MM PCs: (i) bone marrow biopsy section showing asynchronous type MM cells (hematoxylin and eosin; original magnification $\times 500$); (ii) $CD20^+$ MM cells (original magnification $\times 100$; inset, original magnification $\times 500$); (iii) biopsy from a patient with mixed asynchronous and Marschalko-type MM cells (hematoxylin and eosin; original magnification $\times 500$); and (iv) $CD20^+$ single lymphocyte and $CD20^-$ MM cells (original magnification $\times 200$). *CD20* immunohistochemistry was examined without knowledge of clinical history or gene expression findings.

Figure 4. Gene expression correlates with protein expression. Gene and protein expression of CD markers known to be differentially expressed during B-cell differentiation were compared between the MM cell line CAG (left panel) and the EBV-transformed B-lymphoblastoid line ARH-77 (right panel). In both panels, the 8 CD markers are listed in the left column of each panel. Flow cytometric analysis of protein expression is presented in the second column; the AD and AC values of gene expression, in the third and fourth columns. Note the strong expression of both the gene and protein for CD138 and CD38 in the CAG cells but the low expression in the ARH-77 cells. The opposite correlation is observed for the remaining markers.



The progression of MM as a hypoproliferative tumor is thought to be linked to a defect in programmed cell death rather than rapid cell replication.³¹ Two genes, prohibitin (*PHB*) and quiescin Q6 (*QSCN6*), overexpressed in MM are involved in growth arrest. The overexpression of these genes may be responsible for the typically low proliferation indices seen in MM. It is hence conceivable that therapeutic down-regulation of these genes possibly resulting in enhanced proliferation could render MM cells more susceptible to cell cycle–active chemotherapeutic agents.

The gene coding for CD27, *TNFRSF7*, the second most significantly underexpressed gene in MM, is a member of the TNFR superfamily that provides costimulatory signals for T- and B-cell proliferation and B-cell immunoglobulin production and apoptosis.¹⁸ Anti-CD27 significantly inhibits the induction of Blimp-1 and J-chain transcripts, which are turned on in cells committed to PC differentiation,¹⁹ suggesting that ligation of CD27 on B cells may prevent terminal differentiation. CD27 ligand (CD70) prevents apoptosis mediated by interleukin 10 (IL-10) and directs differentiation of CD27⁺ memory B cells toward PCs in cooperation with IL-10.¹⁷ Thus, it is possible that the down-regulation of CD27 gene expression in MM may block an apoptotic program.

The overexpression of CD47 on MM may be related to escape of MM cells from immune surveillance. Studies have shown that cells lacking CD47 are rapidly cleared from the bloodstream by splenic red pulp macrophages and CD47 on normal red blood cells prevents this elimination.³²

The gene product of DNA methyltransferase 1, *DNMT1*, overexpressed in MM, is responsible for cytosine methylation in mammals and has an important role in epigenetic gene silencing. In fact, aberrant hypermethylation of tumor suppressor genes plays an important role in the development of many tumors (for a review, see Baylin³³). De novo methylation of *p16/INK4a* is a frequent finding in primary MM.^{34,35} Also, recent studies have shown that up-regulated expression of *DNMTs* may contribute to the pathogenesis of leukemia by inducing aberrant regional hypermethylation.³⁶ DNA methylation represses genes partly by recruitment of the methyl-CpG-binding protein MeCP2, which in turn recruits a histone deacetylase activity. Fuks et al³⁷ have shown that the process of DNA methylation, mediated by *Dnmt1*, may depend on or generate an altered chromatin state via histone deacetylase activity. It is potentially significant that MM cases also demonstrate significant overexpression of the gene for metastasis-associated 1 (*MTA1*). *MTA1* was originally identified as being highly expressed in metastatic cells.³⁸ *MTA1* has more recently been discovered to be one subunit of the nucleosome remodeling and histone deacetylation (NURD) complex, which contains not only ATP-dependent nucleosome disruption activity, but also histone deacetylase activity.³⁹ Thus, overexpression of *DNMT1* and *MTA1* may have dramatic effects on repressing gene expression in MM.

Oncogenes activated in MM included *ABL* and *MYC*. Although it is not clear whether ABL tyrosine kinase activity is present in MM, it is important to note that overexpression of *abl* and *c-myc* results in the accelerated development of mouse plasmacytomas.⁴⁰ Thus, it may be more than a coincidence that MM cells significantly overexpress *MYC* and *ABL*. Chromosomal translocations involving the *MYC* oncogene and *IGH* and *IGL* genes, resulting in dysregulated *MYC* expression, are hallmarks of Burkitt lymphoma⁴¹ and experimentally induced mouse plasmacytomas⁴²; however, *MYC/IGH*-associated translocations are rare in MM.^{43,44} Although high *MYC* expression was a common feature in our panel

of MM, it was quite variable, ranging from little or no expression to highly elevated expression. It is also of note that the *MAZ* gene whose product is known to bind to and activate *MYC* expression was significantly up-regulated in the MM4 subgroup. Given the important role of *MYC* in B-cell neoplasia, we speculate that overexpression of *MYC*, and possibly *ABL*, in MM may have biologic and possibly prognostic significance.

EXT1 and *EXT2*, which are tumor suppressor genes involved in hereditary multiple exostoses,⁴⁵ heterodimerize and are critical in the synthesis and display of cell surface heparan sulfate glycosaminoglycans (GAGs).^{46,47} *EXT1* is expressed in both MM and normal PCs. *EXT2L* was overexpressed in MM, suggesting that a functional glycosyltransferase could be created in MM. It is of note that syndecan-1 (*CD138/SDC1*), a transmembrane heparan sulfate proteoglycan, is abundantly expressed on MM cells and, when shed into the serum, is a negative prognostic factor.⁴⁸ Thus, abnormal GAG-modified SDC1 may be important in MM biology. The link of SDC1 to MM biology is furthered by the recent association of SDC1 in the signaling cascade induced by the WNT proto-oncogene products. Alexander et al⁴⁹ showed that syndecan-1 (SDC1) is required for Wnt-1–induced mammary tumorigenesis. We observed significant down-regulation of *WNT10B* in primary MM cases. It is also of note that the *WNT5A* gene and the *FRZB* gene, which codes for a decoy WNT receptor,^{50,51} were also marginally up-regulated in newly diagnosed MM (J.S., unpublished data, May 2001). Given that the WNTs represent a novel class of B-cell regulators,^{52,53} deregulation of the expression of these growth factors (*WNT5A*, *WNT10B*) and their receptors (eg, *FRZB*) and gene products that modulate receptor signaling (eg, *SDC1*), may be important in the genesis of MM.

In addition to identifying genes that were statistically different between the group of normal PCs and MM PCs, we also identified genes, like *FGFR3* and *CCND1*, that demonstrate highly elevated “spiked” expression in subsets of MMs. Patients with elevated expression of these genes can have significant distribution differences among the 4 gene expression cluster subgroups. For example, *FGFR3* spikes are found in MM1 and MM2, whereas spikes of *IFI27* are more likely to be found in MM3 and MM4. Highly elevated expression of the interferon-induced gene, *IFI27*, may be indicative of a viral infection, either systemic or specifically within the PCs from these patients, as correlation analysis has shown that *IFI27* spikes are significantly linked (Pearson correlation coefficient values of .77 to .60) to elevated expression of 14 interferon-induced genes, including *MX1*, *MX2*, *OAS1*, *OAS2*, *IFIT1*, *IFIT4*, *PLSCR1*, and *STAT1* (J.S., unpublished data, May 2001). More recent analysis of a large population of MM patients (n = 280), indicated that nearly 25% of all patients had spikes of the *IFI27* gene, thus including a large percentage of patients (J.S., unpublished data, May 2001). Studies are now ongoing that are investigating (1) whether or not the patients showing the *IFI27* spike who cluster in the MM4 subgroup are more likely to have a poor clinical course and (2) to identify the suspected viral infection causing the up-regulation of this class of genes. Thus, spiked gene expression may also be used in the development of clinically relevant prognostic groups.

Finally, the 100% coincidence of spiked *FGFR3* or *CCND1* gene expression with the presence of the t(4;14)(p14;q32) or t(11;14)(q13;q32) translocations as well as the strong correlations between protein expression and gene expression represent important validations of the accuracy of gene expression profiling and

suggests that gene expression profiling may eventually supplant the labor intensive and expensive clinical laboratory procedures, such as cell surface marker immunophenotyping and molecular and cellular cytogenetics.

Because cancer is thought to arise from permanent alterations in gene expression, our comparison of global gene expression patterns in normal and malignant PCs provides a snapshot of the genetic abnormalities that create the malignant MM phenotype. Many of the genes known to be involved in myeloma genesis, for example, *CCND1*, *FGFR3*, *MYC*, *HGF*, and *MVP*, were identified by high-density oligonucleotide DNA microarray comparison of normal and malignant PCs. Importantly, an abundance of heretofore unrecognized classes of genes have been discovered that may be intimately involved in the malignant transformation of PCs and should provide a new framework for studying MM molecular and cellular biology. Similar to investigations in leukemia⁵⁴ and lymphoma,⁵⁵ gene expression profiling is anticipated to result in the

identification of distinct and prognostically relevant clinical subgroups of MM. Recognition of new therapeutic targets, for example, farnesyltransferase and proteasome components, may lead to a rational design of tumor-specific therapies.

Acknowledgments

We would like to thank members of the Lambert Laboratory, Jena Derrick, Ailian Li, Kelly McCastlain, Ruston Smith, Elizabeth Williamson, Yan Xiao, and Hongwei Xu for technical assistance without which this project would not have been possible. We thank the MIRT staff, especially Clyde Bailey and Randell Terry for data management; Joth Jacobson and Trey Spencer for statistical support; and P. L. Bergsagel for advice on RT-PCR experimental design; and Paula Card-Higginson for technical writing and editorial assistance.

References

- Barlogie B, Shaughnessy J, Munshi N, Epstein J. Plasma cell myeloma. In Beutler E, Lichtman M, Coller B, Kipps T, Seligsohn U, eds. *Williams Hematology*. 6th ed. New York, NY: McGraw-Hill; 2001:1279-1304.
- Drach J, Schuster J, Nowotny H, et al. Multiple myeloma: high incidence of chromosomal aneuploidy as detected by interphase fluorescence in situ hybridization. *Cancer Res*. 1995;55:3854-3859.
- Latreille J, Barlogie B, Johnston D, Drewinko B, Alexanian R. Ploidy and proliferative characteristics in monoclonal gammopathies. *Blood*. 1982;59:43-51.
- Sawyer JR, Waldron JA, Jagannath S, Barlogie B. Cytogenetic findings in 200 patients with multiple myeloma. *Cancer Genet Cytogenet*. 1995;82:41-49.
- Dewald GW, Kyle RA, Hicks GA, Greipp PR. The clinical significance of cytogenetic studies in 100 patients with multiple myeloma, plasma cell leukemia, or amyloidosis. *Blood*. 1985;66:380-390.
- Tricot G, Barlogie B, Jagannath S, et al. Poor prognosis in multiple myeloma is associated only with partial or complete deletions of chromosome 13 or abnormalities involving 11q and not with other karyotype abnormalities. *Blood*. 1995;86:4250-4256.
- Desikan R, Barlogie B, Sawyer J, et al. Results of high-dose therapy for 1000 patients with multiple myeloma: durable complete remissions and superior survival in the absence of chromosome 13 abnormalities. *Blood*. 2000;95:4008-4010.
- Seong C, Delasalle K, Hayes K, et al. Prognostic value of cytogenetics in multiple myeloma. *Br J Haematol*. 1998;101:189-194.
- Greipp PR, Katzmann JA, O'Fallon WM, Kyle RA. Value of beta 2-microglobulin level and plasma cell labeling indices as prognostic factors in patients with newly diagnosed myeloma. *Blood*. 1988;72:219-223.
- Bataille R, Boccadoro M, Klein B, Durie B, Pileri A. C-reactive protein and beta-2 microglobulin produce a simple and powerful myeloma staging system. *Blood*. 1992;80:733-737.
- Greipp PR, Lust JA, O'Fallon WM, Katzmann JA, Witzig TE, Kyle RA. Plasma cell labeling index and beta 2-microglobulin predict survival independent of thymidine kinase and C-reactive protein in multiple myeloma. *Blood*. 1993;81:3382-3387.
- Shaughnessy J, Tian E, Sawyer J, et al. High incidence of chromosome 13 deletion in multiple myeloma detected by multiprobe interphase FISH. *Blood*. 2000;96:1505-1511.
- Zojer N, Konigsberg R, Ackermann J, et al. Deletion of 13q14 remains an independent adverse prognostic variable in multiple myeloma despite its frequent detection by interphase fluorescence in situ hybridization. *Blood*. 2000;95:1925-1930.
- Facon T, Avet-Loiseau H, Guillemin G, et al. Chromosome 13 abnormalities identified by FISH analysis and serum beta2-microglobulin produce a powerful myeloma staging system for patients receiving high-dose therapy. *Blood*. 2001;97:1566-1571.
- Lipshutz RJ, Fodor SP, Gingeras TR, Lockhart DJ. High density synthetic oligonucleotide arrays. *Nat Genet*. 1999;21:20-24.
- Eisen MB, Spellman PT, Brown PO, Botstein D. Cluster analysis and display of genome-wide expression patterns. *Proc Natl Acad Sci U S A*. 1998;95:14863-14868.
- Agematsu K, Nagumo H, Oguchi Y, et al. Generation of plasma cells from peripheral blood memory B cells: synergistic effect of interleukin-10 and CD27/CD70 interaction. *Blood*. 1998;91:173-180.
- Prasad KV, Ao Z, Yoon Y, et al. CD27, a member of the tumor necrosis factor receptor family, induces apoptosis and binds to Siva, a proapoptotic protein. *Proc Natl Acad Sci U S A*. 1997;94:6346-6351.
- Raman VS, Bal V, Rath S, George A. Ligation of CD27 on murine B cells responding to T-dependent and T-independent stimuli inhibits the generation of plasma cells. *J Immunol*. 2000;165:6809-6815.
- Devireddy LR, Teodoro JG, Richard FA, Green MR. Induction of apoptosis by a secreted lipocalin that is transcriptionally regulated by IL-3 deprivation. *Science*. 2001;293:829-834.
- Borset M, Hjorth-Hansen H, Seidel C, Sundan A, Waage A. Hepatocyte growth factor and its receptor c-met in multiple myeloma. *Blood*. 1996;88:3998-4004.
- Chesi M, Nardini E, Brents LA, et al. Frequent translocation t(4;14)(p16.3;q32.3) in multiple myeloma is associated with increased expression and activating mutations of fibroblast growth factor receptor 3. *Nat Genet*. 1997;16:260-264.
- Bathe OF, Franceschi D, Livingstone AS, Moffat FL, Tian E, Ardalan B. Increased thymidylate synthase gene expression in liver metastases from colorectal carcinoma: implications for chemotherapeutic options and survival. *Cancer J Sci Am*. 1999;5:34-40.
- Rinaldi T, Ricci C, Porro D, Bolotin-Fukuhara M, Frontali L. A mutation in a novel yeast proteasomal gene, RPN11/MPR1, produces a cell cycle arrest, overreplication of nuclear and mitochondrial DNA, and an altered mitochondrial morphology. *Mol Biol Cell*. 1998;9:2917-2931.
- Spataro V, Toda T, Craig R, et al. Resistance to diverse drugs and ultraviolet light conferred by overexpression of a novel human 26 S proteasome subunit. *J Biol Chem*. 1997;272:30470-30475.
- Raaijmakers HG, Izquierdo MA, Lokhorst HM, et al. Lung-resistance-related protein expression is a negative predictive factor for response to conventional low but not to intensified dose alkylating chemotherapy in multiple myeloma. *Blood*. 1998;91:1029-1036.
- Li W, Hesabi B, Babbo A, et al. Regulation of double-strand break-induced mammalian homologous recombination by UBL1, a RAD51-interacting protein. *Nucleic Acids Res*. 2000;28:1145-1153.
- Shen Z, Pardington-Purtymun PE, Comeaux JC, Moyzis RK, Chen DJ. Associations of UBE2L with RAD52, UBL1, p53, and RAD51 proteins in a yeast two-hybrid system. *Genomics*. 1996;37:183-186.
- Shen Z, Pardington-Purtymun PE, Comeaux JC, Moyzis RK, Chen DJ. UBL1, a human ubiquitin-like protein associating with human RAD51/RAD52 proteins. *Genomics*. 1996;36:271-279.
- Chen A, Mannen H, Li SS. Characterization of mouse ubiquitin-like SMT3A and SMT3B cDNAs and gene/pseudogenes. *Biochem Mol Biol Int*. 1998;46:1161-1174.
- Hallek M, Bergsagel PL, Anderson KC. Multiple myeloma: increasing evidence for a multistep transformation process. *Blood*. 1998;91:3-21.
- Oldenborg PA, Zheleznyak A, Fang YF, Lagenaur CF, Gresham HD, Lindberg FP. Role of CD47 as a marker of self on red blood cells. *Science*. 2000;288:2051-2054.
- Baylin SB. Tying it all together: epigenetics, genetics, cell cycle, and cancer. *Science*. 1997;277:1948-1949.
- Ng MH, Chung YF, Lo KW, Wickham NW, Lee JC, Huang DP. Frequent hypermethylation of p16 and p15 genes in multiple myeloma. *Blood*. 1997;89:2500-2506.
- Gonzalez M, Mateos MV, Garcia-Sanz R, et al. De novo methylation of tumor suppressor gene p16/INK4a is a frequent finding in multiple myeloma patients at diagnosis. *Leukemia*. 2000;14:183-187.
- Mizuno S, Chijiwa T, Okamura T, et al. Expression of DNA methyltransferases DNMT1, 3A, and 3B

- in normal hematopoiesis and in acute and chronic myelogenous leukemia. *Blood*. 2001;97:1172-1179.
37. Fuks F, Burgers WA, Brehm A, Hughes-Davies L, Kouzarides T. DNA methyltransferase Dnmt1 associates with histone deacetylase activity. *Nat Genet*. 2000;24:88-91.
 38. Toh Y, Pencil SD, Nicolson GL. A novel candidate metastasis-associated gene, mta1, differentially expressed in highly metastatic mammary adenocarcinoma cell lines. cDNA cloning, expression, and protein analyses. *J Biol Chem*. 1994;269:22958-22963.
 39. Xue Y, Wong J, Moreno GT, Young MK, Cote J, Wang W. NURD, a novel complex with both ATP-dependent chromatin-remodeling and histone deacetylase activities. *Mol Cell*. 1998;2:851-861.
 40. Largaespada DA, Kaehler DA, Mishak H, et al. A retrovirus that expresses v-abl and c-myc oncogenes rapidly induces plasmacytomas. *Oncogene*. 1992;7:811-819.
 41. Dalla-Favera R, Bregni M, Erikson J, Patterson D, Gallo RC, Croce CM. Human c-myc onc gene is located on the region of chromosome 8 that is translocated in Burkitt lymphoma cells. *Proc Natl Acad Sci U S A*. 1982;79:7824-7827.
 42. Potter M. Perspectives on the origins of multiple myeloma and plasmacytomas in mice. *Hematol Oncol Clin North Am*. 1992;6:211-223.
 43. Shou Y, Martelli ML, Gabrea A, et al. Diverse karyotypic abnormalities of the c-myc locus associated with c-myc dysregulation and tumor progression in multiple myeloma. *Proc Natl Acad Sci U S A*. 2000;97:228-233.
 44. Kuehl WM, Brents LA, Chesi M, Huppi K, Bergsagel PL. Dysregulation of c-myc in multiple myeloma. *Curr Top Microbiol Immunol*. 1997;224:277-282.
 45. Stickens D, Clines G, Burbee D, et al. The EXT2 multiple exostoses gene defines a family of putative tumour suppressor genes. *Nat Genet*. 1996;14:25-32.
 46. McCormick C, Leduc Y, Martindale D, et al. The putative tumour suppressor EXT1 alters the expression of cell-surface heparan sulfate. *Nat Genet*. 1998;19:158-161.
 47. McCormick C, Duncan G, Goutsos KT, Tufaro F. The putative tumor suppressors EXT1 and EXT2 form a stable complex that accumulates in the Golgi apparatus and catalyzes the synthesis of heparan sulfate. *Proc Natl Acad Sci U S A*. 2000;97:668-673.
 48. Seidel C, Sundan A, Hjorth M, et al. Serum syndecan-1: a new independent prognostic marker in multiple myeloma. *Blood*. 2000;95:388-392.
 49. Alexander CM, Reichsman F, Hinkes MT, et al. Syndecan-1 is required for Wnt-1-induced mammary tumorigenesis in mice. *Nat Genet*. 2000;25:329-332.
 50. Leyns L, Bouwmeester T, Kim SH, Piccolo S, De Robertis EM. Frzb-1 is a secreted antagonist of Wnt signaling expressed in the Spemann organizer. *Cell*. 1997;88:747-756.
 51. Rattner A, Hsieh JC, Smallwood PM, et al. A family of secreted proteins contains homology to the cysteine-rich ligand-binding domain of frizzled receptors. *Proc Natl Acad Sci U S A*. 1997;94:2859-2863.
 52. Reya T, O'Riordan M, Okamura R, et al. Wnt signaling regulates B lymphocyte proliferation through a LEF-1 dependent mechanism. *Immunity*. 2000;13:15-24.
 53. Van Den Berg DJ, Sharma AK, Bruno E, Hoffman R. Role of members of the Wnt gene family in human hematopoiesis. *Blood*. 1998;92:3189-3202.
 54. Golub TR, Slonim DK, Tamayo P, et al. Molecular classification of cancer: class discovery and class prediction by gene expression monitoring. *Science*. 1999;286:531-537.
 55. Alizadeh AA, Eisen MB, Davis RE, et al. Distinct types of diffuse large B-cell lymphoma identified by gene expression profiling. *Nature*. 2000;403:503-511.